Seismic structure, Gravity anomalies and Flexure along the Emperor Seamount chain

A. B. Watts[1*], I. Grevemeyer[2], D. J. Shillington[3], R. A. Dunn[4], B. Boston[5], L. Gómez de la Peña[2]

[1]Department of Earth Sciences, University of Oxford, Oxford, UK
[2]GEOMAR Helmholtz Centre for Ocean Research, Kiel, Germany
[3]School of Earth and Sustainability, Northern Arizona University, Flagstaff, AZ, USA
[4]Department of Earth Sciences, School of Ocean and Earth Science and Technology, University of Hawaii, Honolulu, HI, USA
[5]Lamont Doherty Earth Observatory of Columbia University, Palisades, NY, USA

Supporting Information

Table of Contents

Ocean Bottom Seismometer data

Ocean Bottom Seismometer (OBS) wide-angle reflection and refraction data were acquired using a 4-string, 36-element, 6600 cu. in. air gun array and twenty-nine OBS deployed along MGL1902 Line 2. Three types of OBS with different depth ratings were used, which was necessary given the very large water depths (>6000 m) in the survey area. We used 8 OBS from Woods Hole Oceanographic Institute (WHOI), which are rated to 5500 m, 12 GEOMAR LOBSTERs, which are rated to 6000, and 9 GEOMAR ultradeep LOBSTERs, which are rated to 8000 m. Further details on the ultradeep instruments can be found in *Grevemeyer and Flueh* [2008]. The gun array was towed at a depth of 12 m and a nominal shot spacing of 400 m (equivalent to a shot interval of 194 s at 4 knots) was selected in order to minimize previous shot noise due to the shallower water depths and possible unsedimented tops of Jimmu and Suiko guyots. The WHOI data were processed to SEGY and the GEOMAR data were processed to MINISEED, SAC and SEGY. Basic processing steps were applied to these data: bandpass filtering, offset dependent gains and trace balancing, reduction velocities.

Examples of OBS record sections are shown in Figs. S1-S8. The figures were constructed in GMT 4 [*Wessel and Luis*, 2017] using `ps2segy`. Coloured lines show observed and predicted travel times based on the *P* wave velocity model in Fig. 4. Green solid lines show observed picks. Red solid lines show calculated first arrival refractions (*Pg* and *Pn*). Blue solid lines show calculated *PmP* wide-angle reflector. Individual OBS stations are located in Fig. 1b.

Multichannel seismic reflection data

MultiChannel Seismic (MCS) reflection acquisition used the same 4-string, 36-element, 6600 cu. in. air gun array that the OBS transect employed. Shots were fired every 62.5 m to an 1188-channel, 14.875-km-long streamer that recorded for a length of 26 s at a sample rate of 2 ms. Both the streamer and the source were towed at a depth of 12 m. Processing of the MCS data included: SEGD import, geometry assignment, low-cut filter (3 Hz), trace edit, resampling to 4 ms, swell and spike reduction, FK filter, static, debias, spherical divergence, 2D surface related multiple attenuation, wave equation multiple attenuation, deconvolution, regularization, parabolic Radon, velocity analysis, 2D Kirchhoff prestack time migration, time-frequency noise suppression, inner and outer mutes, stacking, time-varying bandpass filter beneath the acoustic basement, and a seafloor mute. The starting velocity began with velocity analysis every 250 CMPs that was updated using a horizon-based velocity analysis approach. The OBS-derived *Vp* tomographic models (Figs. 4, 5) was converted into the time domain and merged with the MCS derived velocity model beneath the acoustic basement and used for prestack time migration. Interpreted horizons were picked on the time migrated data and depth converted using only the OBS-derived *Vp* tomographic model.

Examples of the time migrated MCS data are shown in Figs. S9-S13. The figures were constructed in GMT 5 [*Wessel and Luis*, 2017] using `segy2grd` and `grdimage`. Coloured lines show the picks of prominent reflectors which were depth converted and shown in the summary crust and mantle model in Fig. 11

Figure captions:

Fig. S1. OBS record section at GEOMAR LOBSTER Station 203 on unnamed seamount north of Jimmu guyot.

Fig. S2. OBS record section at GEOMAR ultradeep LOBSTER Station 206 on Jimmu guyot.

Fig. S3. OBS record section at GEOMAR ultradeep LOBSTER Station 214.

Fig. S4. OBS record section at GEOMAR LOBSTER Station 218 on Suiko guyot.

Fig. S5. OBS record section at WHOI Station 221 on Suiko guyot.

Fig. S6. OBS record section at GEOMAR ultradeep LOBSTER Station 222 on Suiko guyot.

Fig. S7. OBS record section at WHOI Station 225 on Suiko guyot

Fig. S8. OBS record section at GEOMAR LOBSTER Station 228.

Fig. S9. Time migrated MCS Line 2 across Jimmu and Suiko guyots and an unnamed seamount to the north of Jimmu. Top panel - original data. Bottom panel – original data with reflector picks. Boxes show the expanded plots in Figs. S10-S13.

Fig. S10. Time migrated MCS Line 2 over the deep water between Jimmu guyot and an unnamed seamount to the north.

Fig. S11. Time migrated MCS Line 2 over the deep water between Jimmu and Suiko guyots.

Fig. S12. Time migrated MCS Line 2 over the north flank of Suiko guyot in the region of DSDP Site 433 [*Shipboard Scientific Party*, 1980]. The vertical yellow line shows the position of the site after projection of 5.407 km onto MCS Line 2. The horizontal yellow lines show the sub-surface depth in TWTT of Acoustic units I, II and III based on data in Table 25 of *Shipboard Scientific Party* [1988]. Acoustic units I, II, and III consist mainly of upper/lower Miocene to Recent pelagic oozes, middle to upper Paleocene reef sands and sandy muds, and middle to upper Paleocene of intercalated basaltic lava flows and reef sands respectively.

Fig. S13. Time migrated MCS Line 2 over the south flank of Suiko guyot.

References:

Grevemeyer, I., and E. Flueh (2008), Cruise Report SO195 TOTAL - TOnga Thrust earthquake Asperity at Louisville Ridge ; Suva/Fiji - Suva/Fiji 07.01.-16.02.2008. In: IFM-GEOMAR Report 14, doi: https://doi.org/10.23689/fidgeo-623

Shipboard_Scientific_Party (1980), Site 433: Suiko Seamount, *Deep Sea Drilling Project Reports and Publications*, *LV*, 127-156, doi: https://doi.org/10.2973/dsdp.proc.55.106.1980

Wessel, P., and J. F. Luis (2017), The GMT/MATLAB Toolbox, *Geochemistry Geophysics Geosystems*, *18*, 811-823, doi: https://doi.org/10.1002/2016GC006723

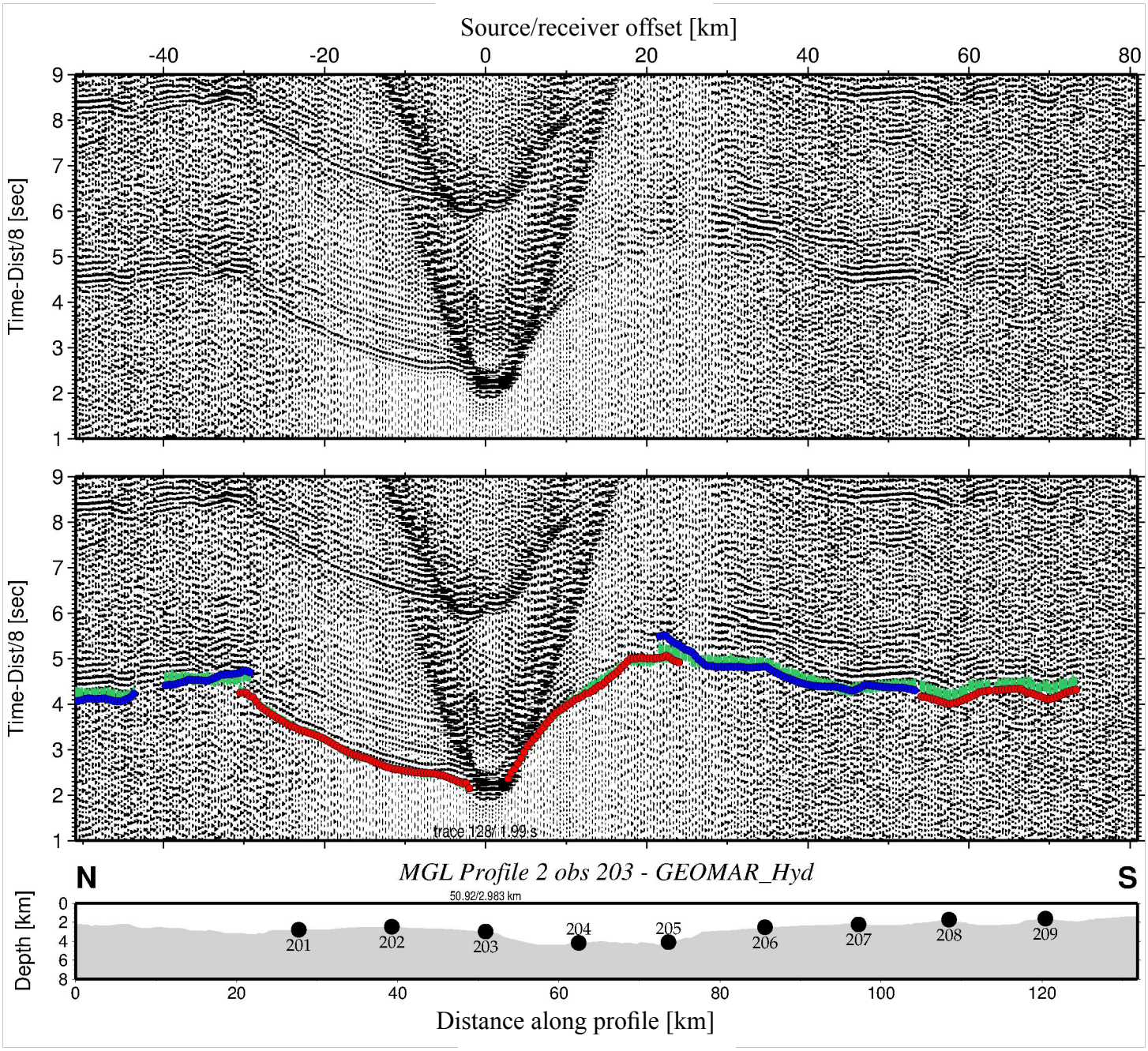
Source/receiver offset [km]
-40
-20
0
20
40
60
80
Time-Dist/8 [sec]
9
8
7
6
5
4
3
2
1
trace 128/ 1.99 s
N
MGL Profile 2 obs 203 - GEOMAR_Hyd
S
50.92/2.983 km
Depth [km]
0
2
4
6
8
201
202
203
204
205
206
207
208
209
0
20
40
60
80
100
120
Distance along profile [km]

Fig. S1

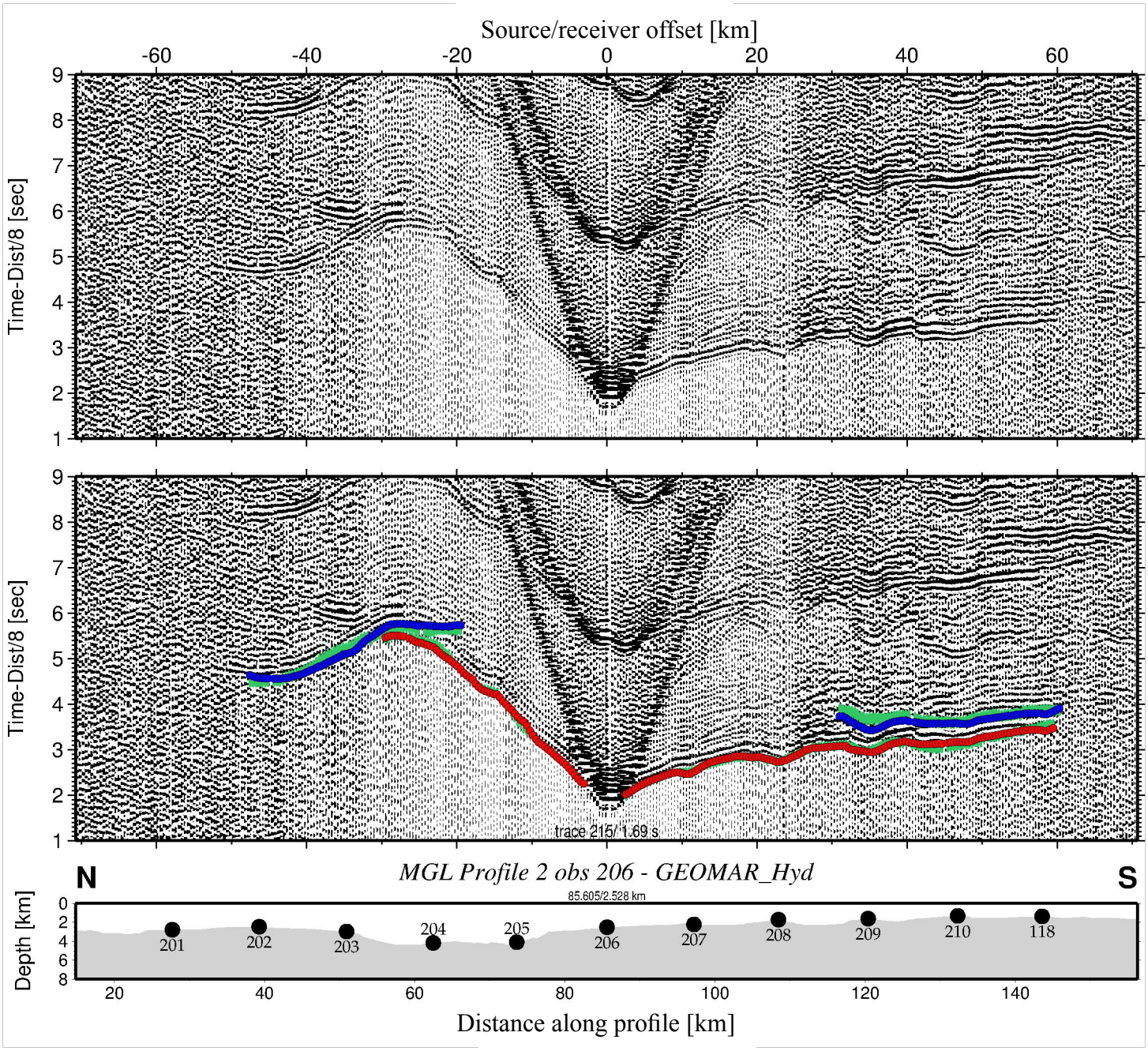
Source/receiver offset [km]
-60
-40
-20
0
20
40
60
Time-Dist/8 [sec]
9
8
7
6
5
4
3
2
1
trace 215/ 1.69 s
N
MGL Profile 2 obs 206 - GEOMAR_Hyd
S
85.605/2.528 km
Depth [km]
0
2
4
6
8
201
202
203
204
205
206
207
208
209
210
118
20
40
60
80
100
120
140
Distance along profile [km]

Fig. S2

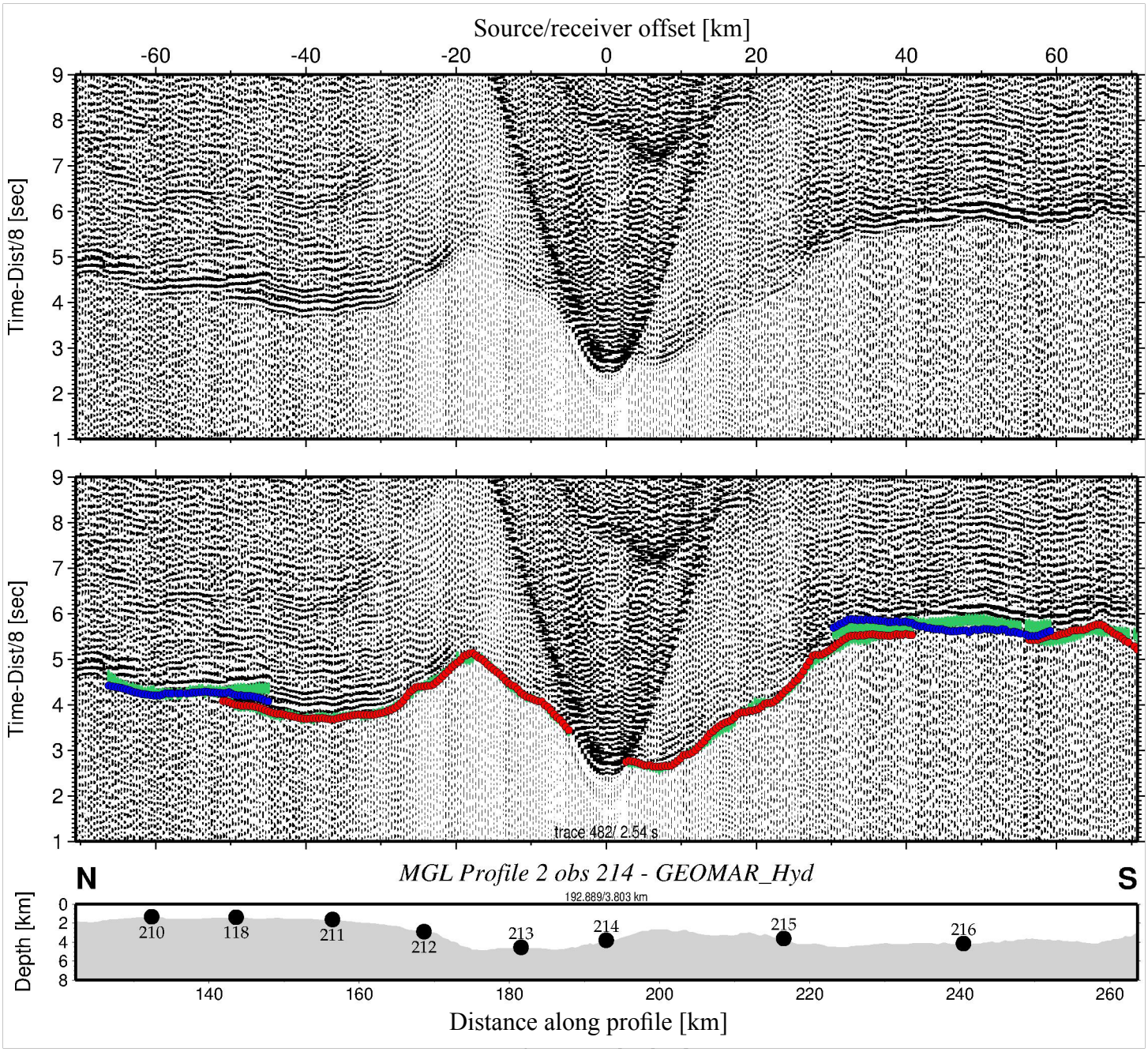
Source/receiver offset [km]
-60
-40
-20
0
20
40
60
Time-Dist/8 [sec]
trace 482/ 2.54 s
N
MGL Profile 2 obs 214 - GEOMAR_Hyd
S
192.889/3.803 km
Depth [km]
210
118
211
212
213
214
215
216
Distance along profile [km]

Fig. S3

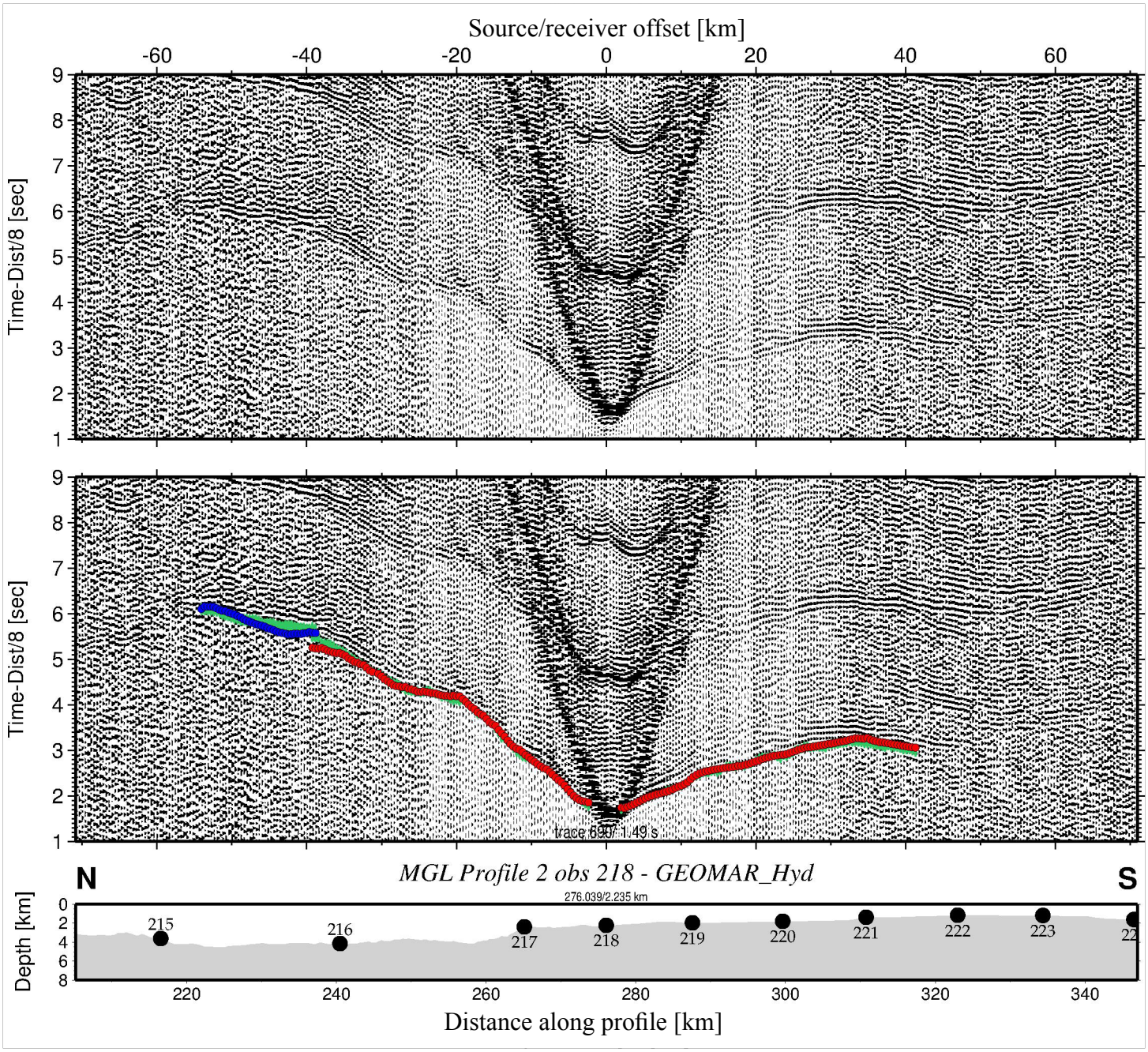
Source/receiver offset [km]
-60
-40
-20
0
20
40
60
Time-Dist/8 [sec]
9
8
7
6
5
4
3
2
1
trace 690/ 1.49 s
N
MGL Profile 2 obs 218 - GEOMAR_Hyd
S
276.039/2.235 km
Depth [km]
0
2
4
6
8
215
216
217
218
219
220
221
222
223
220
240
260
280
300
320
340
Distance along profile [km]

Fig. S4

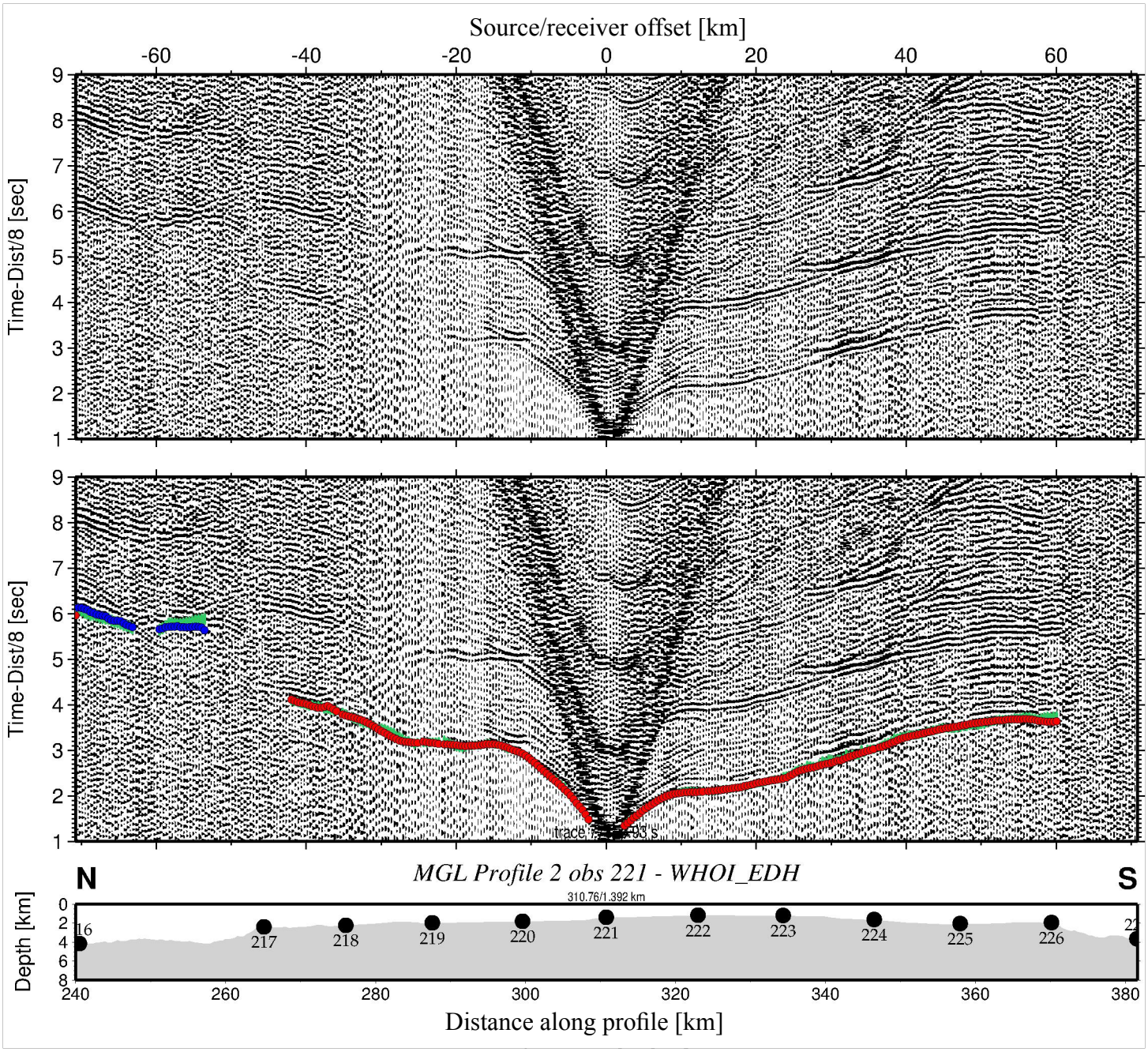
Source/receiver offset [km]
-60
-40
-20
0
20
40
60
Time-Dist/8 [sec]
9
8
7
6
5
4
3
2
1
Time-Dist/8 [sec]
N
MGL Profile 2 obs 221 - WHOI_EDH
S
310.76/1.392 km
Depth [km]
0
2
4
6
8
16
217
218
219
220
221
222
223
224
225
226
240
260
280
300
320
340
360
380
Distance along profile [km]

Fig. S5

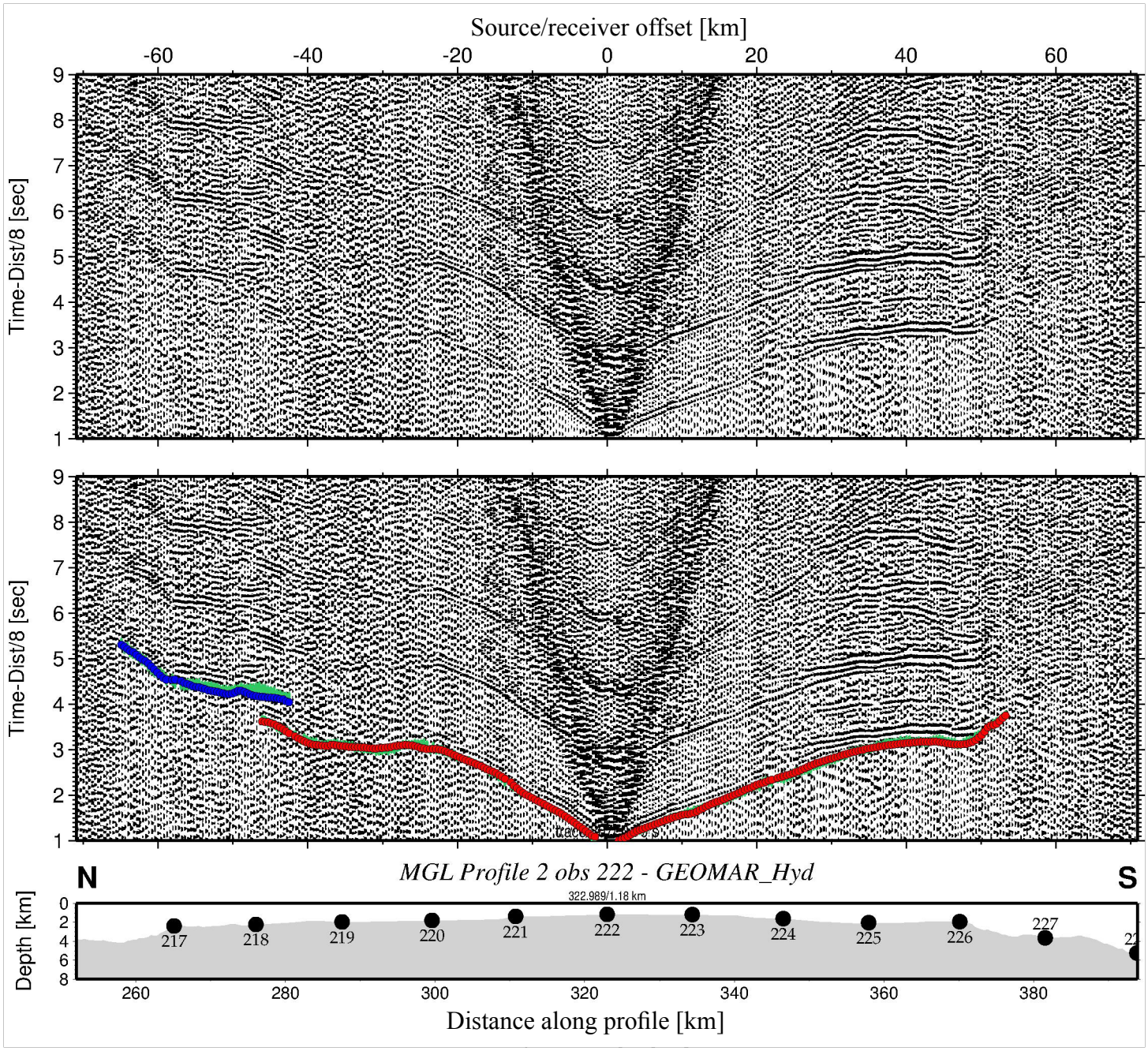
Source/receiver offset [km]
-60
-40
-20
0
20
40
60
Time-Dist/8 [sec]
9
8
7
6
5
4
3
2
1
Time-Dist/8 [sec]
N
MGL Profile 2 obs 222 - GEOMAR_Hyd
S
322.989/1.18 km
Depth [km]
0
2
4
6
8
217
218
219
220
221
222
223
224
225
226
227
260
280
300
320
340
360
380
Distance along profile [km]

Fig. S6

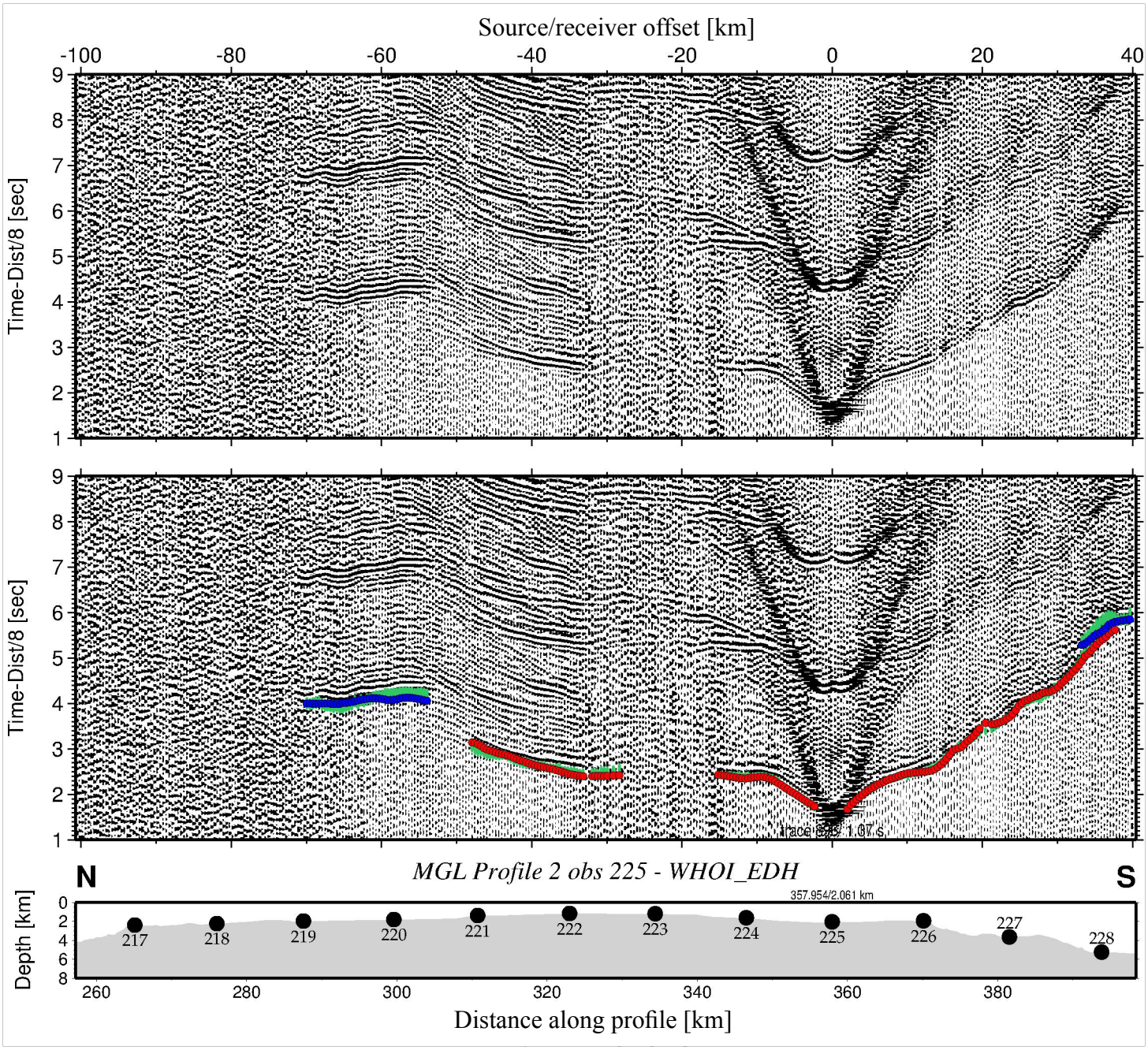
Source/receiver offset [km]
-100
-80
-60
-40
-20
0
20
40
Time-Dist/8 [sec]
9
8
7
6
5
4
3
2
1
Time-Dist/8 [sec]
trace 225 1.67 s
N
MGL Profile 2 obs 225 - WHOI_EDH
S
357.954/2.061 km
Depth [km]
0
2
4
6
8
217
218
219
220
221
222
223
224
225
226
227
228
260
280
300
320
340
360
380
Distance along profile [km]

Fig. S7

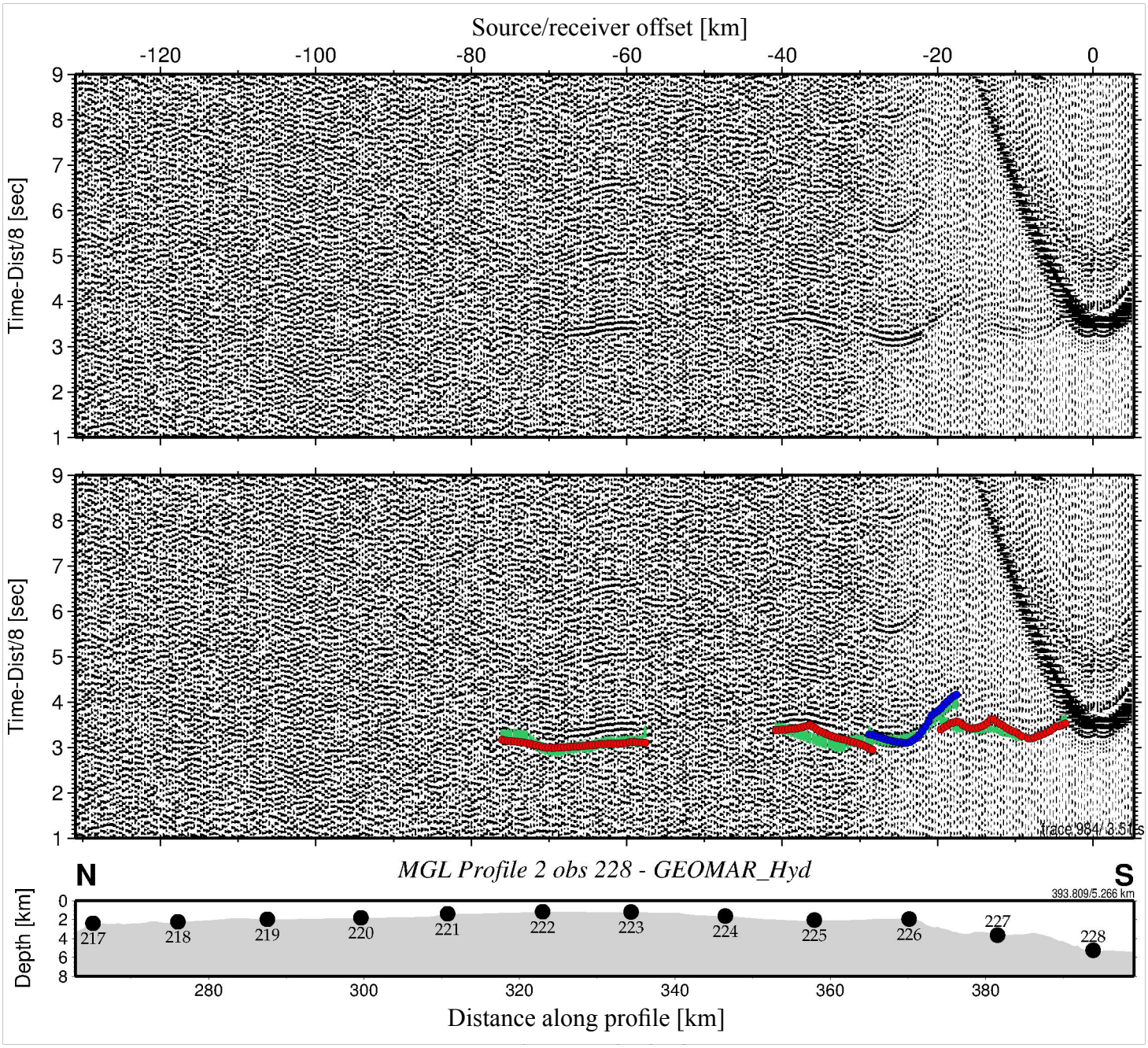
Source/receiver offset [km]
-120
-100
-80
-60
-40
-20
0
Time-Dist/8 [sec]
9
8
7
6
5
4
3
2
1
Time-Dist/8 [sec]
Trace 984/ 3.51s
N
MGL Profile 2 obs 228 - GEOMAR_Hyd
S
393.809/5.266 km
Depth [km]
0
2
4
6
8
217
218
219
220
221
222
223
224
225
226
227
228
280
300
320
340
360
380
Distance along profile [km]

Fig. S8

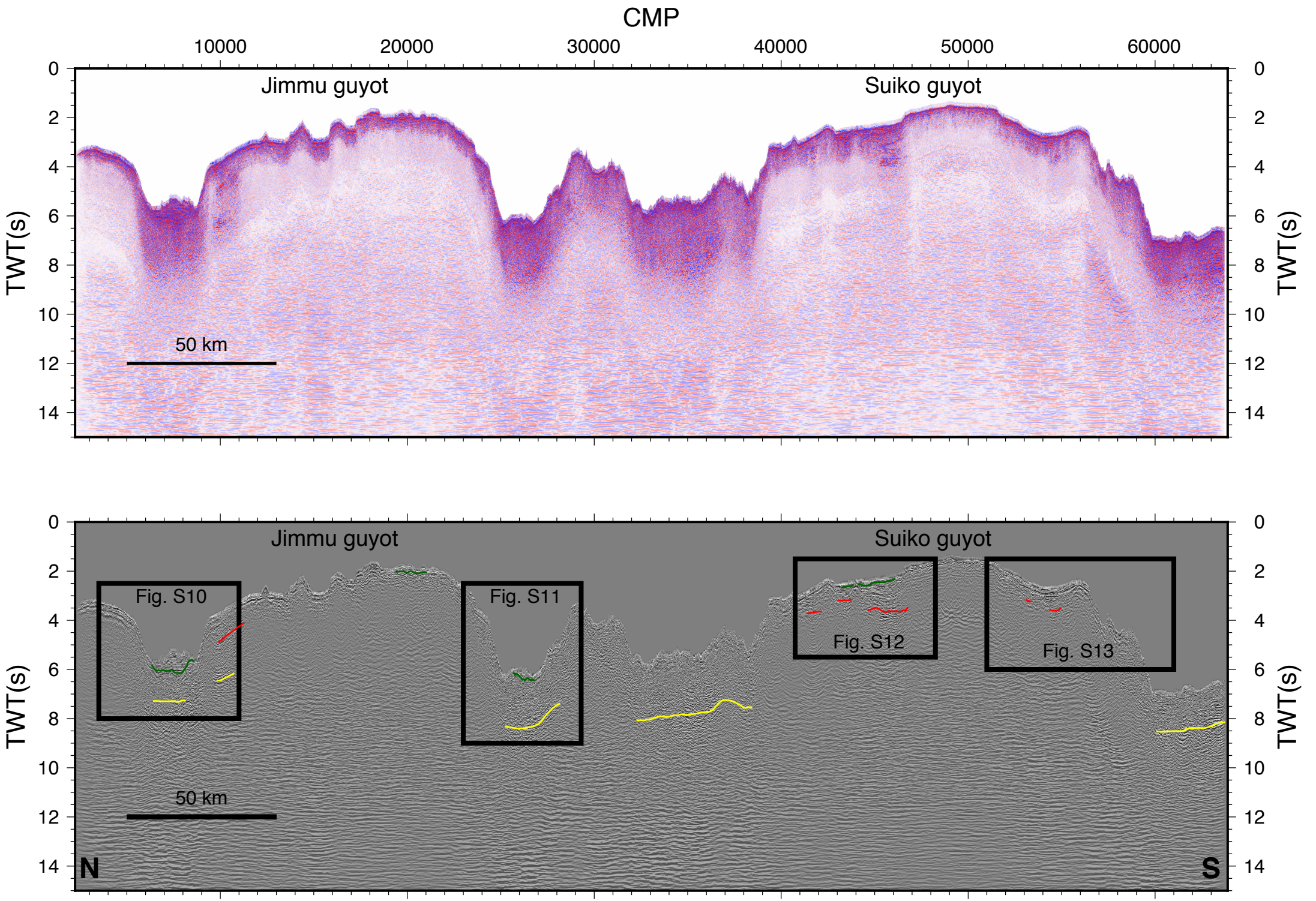
CMP
10000
20000
30000
40000
50000
60000
Jimmu guyot
Suiko guyot
TWT(s)
0
2
4
6
8
10
12
14
50 km
Jimmu guyot
Suiko guyot
Fig. S10
Fig. S11
Fig. S12
Fig. S13
50 km
N
S

Fig. S9

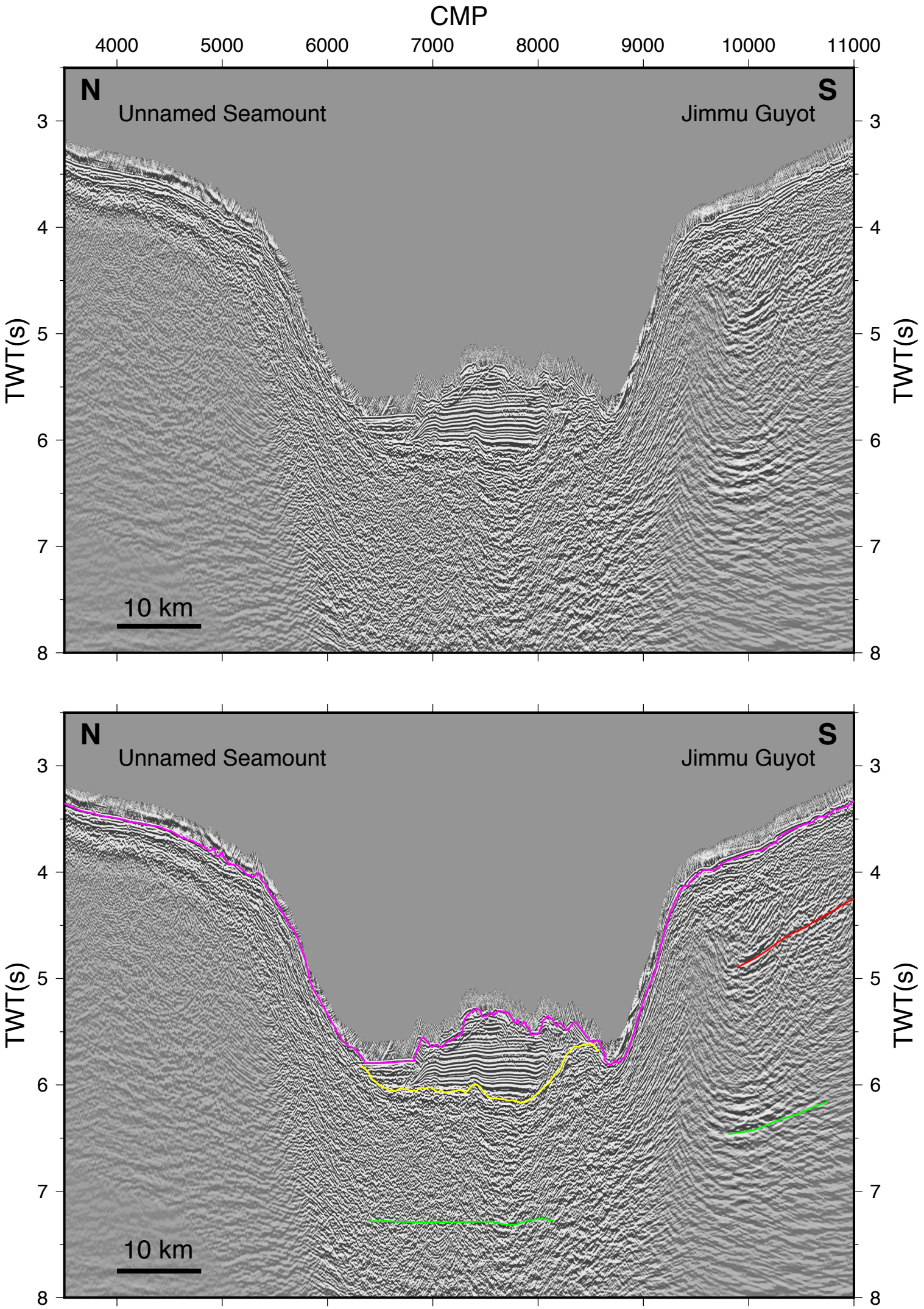
CMP
4000
5000
6000
7000
8000
9000
10000
11000
N
S
Unnamed Seamount
Jimmu Guyot
TWT(s)
3
4
5
6
7
8
10 km
N
S
Unnamed Seamount
Jimmu Guyot
TWT(s)
10 km

Fig. S10

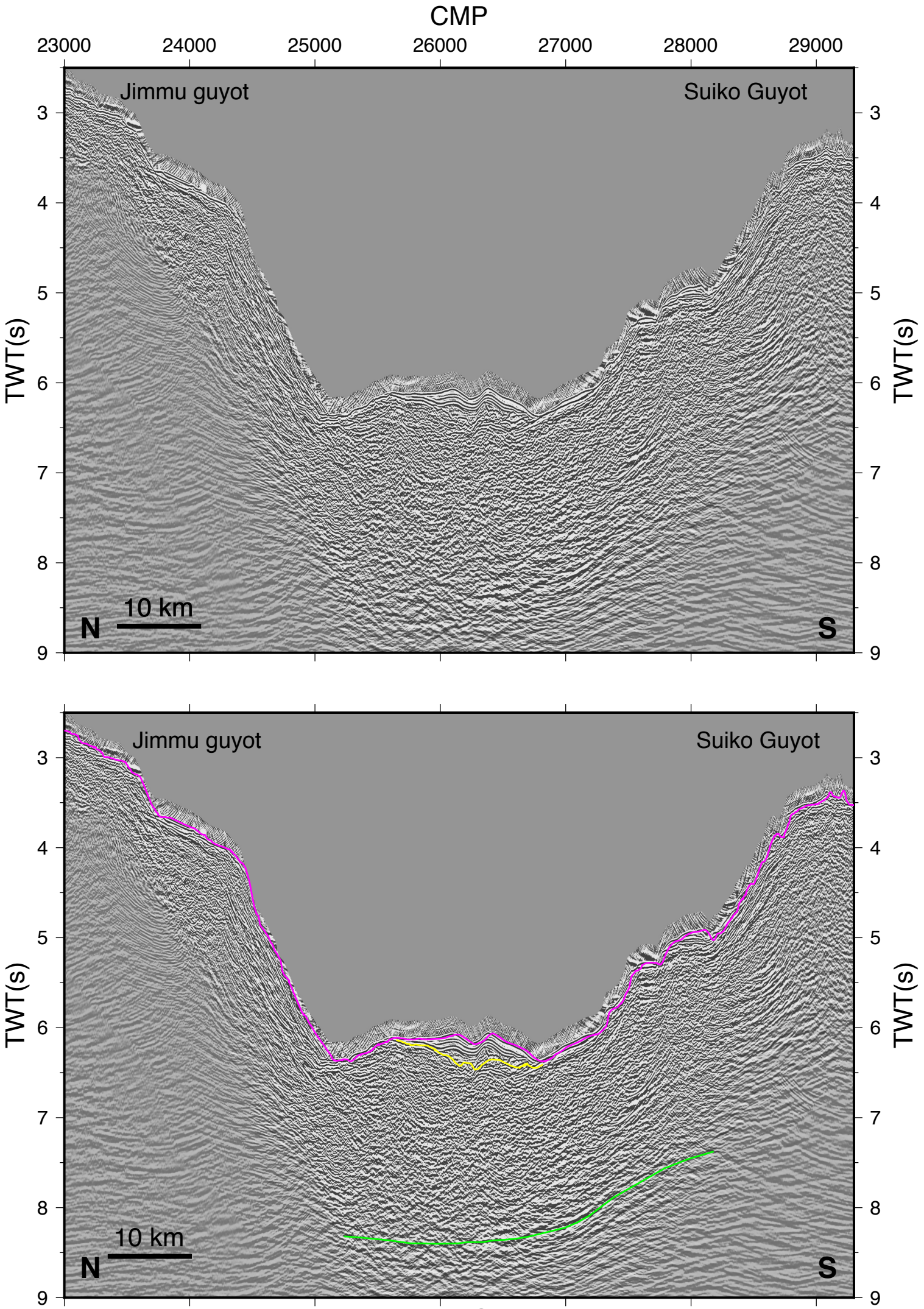
CMP
23000
24000
25000
26000
27000
28000
29000
Jimmu guyot
Suiko Guyot
TWT(s)
3
4
5
6
7
8
9
10 km
N
S
Jimmu guyot
Suiko Guyot
TWT(s)
10 km
N
S

Fig. S11

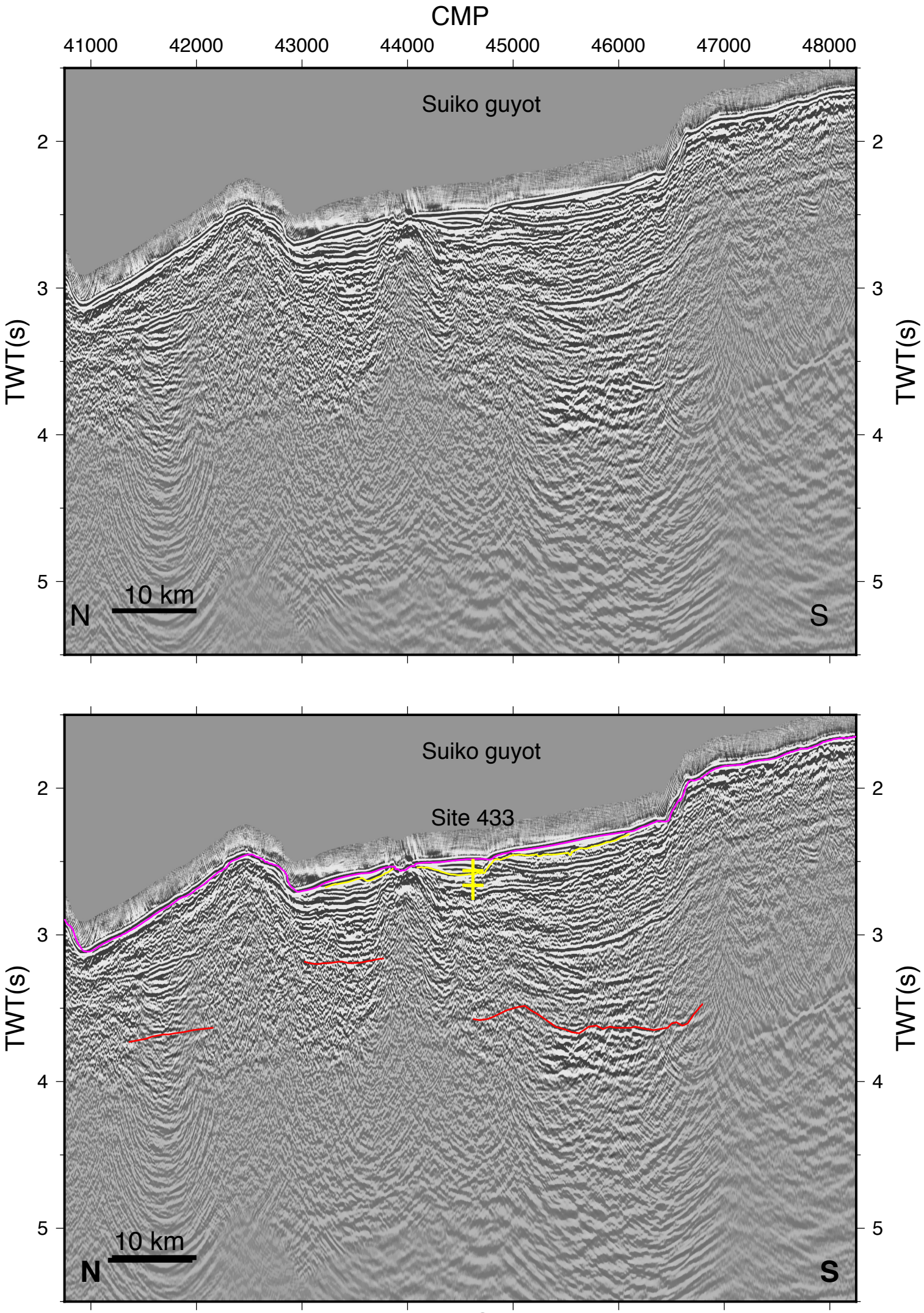
CMP
41000
42000
43000
44000
45000
46000
47000
48000
Suiko guyot
TWT(s)
2
3
4
5
10 km
N
S
Suiko guyot
Site 433
TWT(s)
2
3
4
5
10 km
N
S

Fig. S12

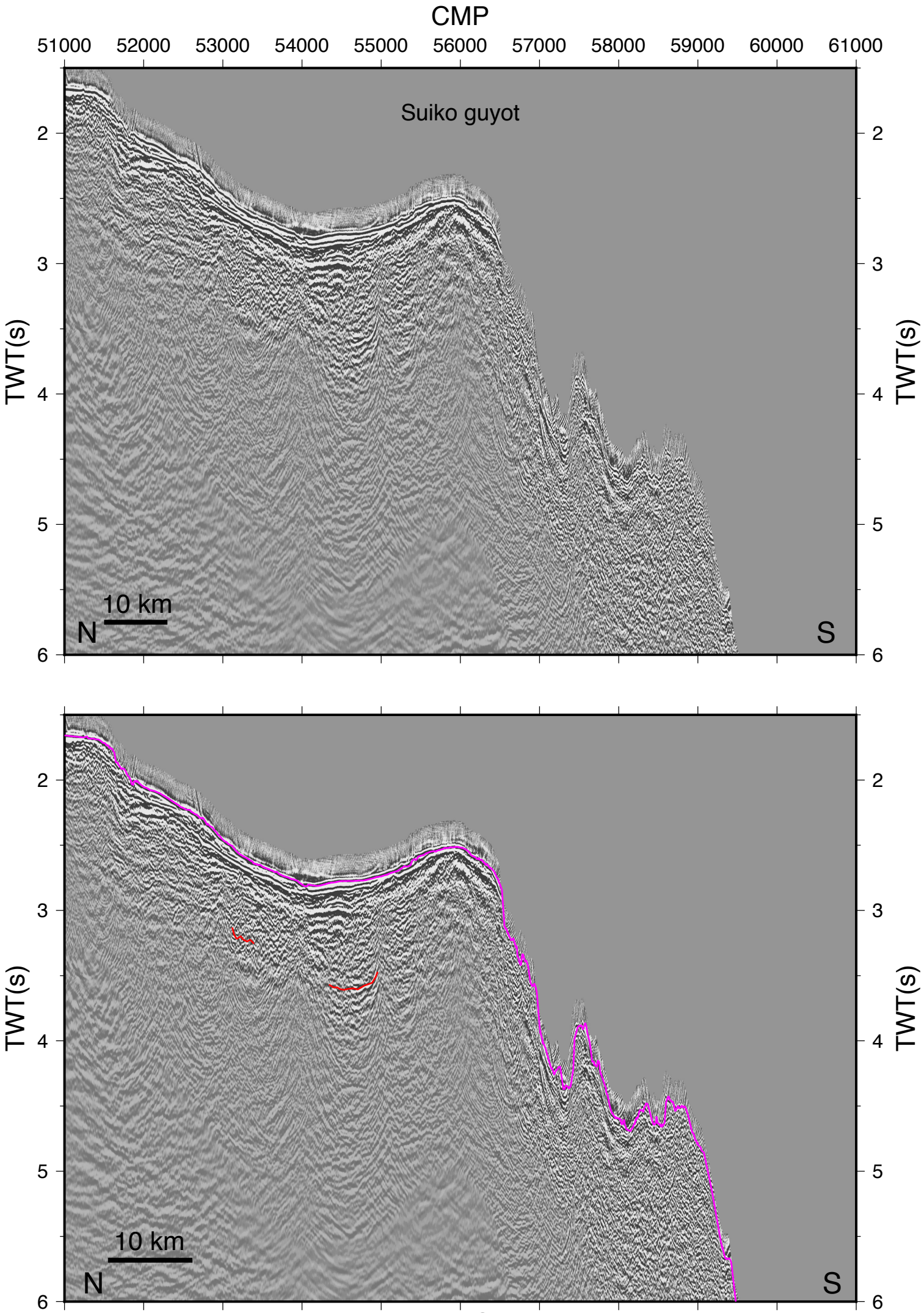
CMP
51000
52000
53000
54000
55000
56000
57000
58000
59000
60000
61000
Suiko guyot
TWT(s)
2
3
4
5
6
10 km
N
S

Fig. S13